

## Supporting Information

### Nano-flowered Ce@MOR hybrids with modulated acid properties for the vapor-phase dehydration of 1,3-butanediol into butadiene

Lin Fang,<sup>[a]\*</sup> Fangli Jing,<sup>[b]</sup> Jingya Lu,<sup>[a]</sup> Bingwen Hu,<sup>[c]</sup> and Marc Pera-Titus<sup>[a]\*</sup>

<sup>a</sup> E2P2L UMI 3464 CNRS – Solvay, 3966 Jin Du Road, Xin Zhuang Ind. Zone, 201108 Shanghai, China

<sup>b</sup> Univ. Lille, CNRS, Centrale Lille, ENSCL, Univ. Artois, UMR 8181 – UCCS, F-59000 Lille, France

<sup>c</sup> School of Chemical Engineering, Sichuan University, 610065 Chengdu, China

<sup>d</sup> School of Physics and Materials Science & Shanghai Key Laboratory of Magnetic Resonance, East China Normal University, 3663 N. Zhongshan Road, Shanghai 200062, China

\*Corresponding author: [lin.fang@solvay.com](mailto:lin.fang@solvay.com), [marc.pera-titus-ext@solvay.com](mailto:marc.pera-titus-ext@solvay.com)

---

## FIGURE CAPTIONS

Figure S1. Evolution of the catalytic performance as a function of the time on stream (TOS) for: (a) MOR, (b) Ce-MOR\_200(IWI), (c) Ce-MOR\_50(IWI), (d) Ce@MOR\_200, (e) Ce@MOR\_100 and (f) Ce@MOR\_50. Nomenclature: X<sub>BDO</sub>, 1,3-BDO conversion; S<sub>BD</sub>, BD selectivity; S<sub>PE</sub>, propylene selectivity; S<sub>3B1ol</sub>, 3B1ol selectivity.

Figure S2. Band deconvolution for DRUV spectra: (a) MOR, (b) Ce-MOR\_200(IWI), (c) Ce@MOR\_200, (d) Ce@MOR\_50, (e) Ce@MOR\_20 and (f) CeO<sub>2</sub>.

Figure S3. TEM-EDX images of Ce@MOR\_50 showing the location of Si (blue), Al (green), Ce (yellow) and O (magenta).

Figure S4. Band deconvolution for Ce 3d XPS spectra: (a) Ce-MOR\_200(IWI), (b) Ce@MOR\_200, (c) Ce-MOR\_50(IWI), (d) Ce@MOR\_50, (e) Ce@MOR\_20 and (f) MOR.

Figure S5. O1s XPS spectra for: (a) Ce-MOR\_20 and (b) Ce@MOR\_50(IWI).

Figure S6. H<sub>2</sub>-TPR profiles for: (a) Ce@MOR\_50(IWI), (b) MOR, (c) Ce@MOR\_200, (d) Ce@MOR\_100, (e) Ce@MOR\_50 and (f) Ce@MOR\_20.

Figure S7. N<sub>2</sub> adsorption/desorption isotherms for: (a) MOR, (b) Ce@MOR\_200, (c) Ce@MOR\_100 and (d) Ce@MOR\_50.

Figure S8. TGA / DTG profiles for the fresh and spent catalysts: (a) fresh MOR, (b) spent MOR, (c) fresh Ce@MOR\_100 and (d) spent Ce@MOR\_100.

Figure S9. FT-IR absorption spectra after pyridine adsorption for: (a) H-MOR, (b)

Ce@MOR\_100 and (c) Ce@MOR\_50.

Figure S10. Deconvoluted  $^{29}\text{Si}$  NMR MAS spectra for: (a) MOR, (b) Ce@MOR\_200, (c) Ce@MOR\_50 and (d) Ce@MOR\_50(IWI).

Figure S11. Deconvoluted NH<sub>3</sub>-TPD profiles for the fresh catalysts: (a) MOR, (b) Ce@MOR\_200, (c) Ce@MOR\_100, (d) Ce@MOR\_50, (e) Ce@MOR\_200(IWI) and (f) Ce@MOR\_50(IWI).

Figure S12. Deconvoluted NH<sub>3</sub>-TPD profiles for the spent catalysts: (a) MOR, (b) Ce@MOR\_100, (c) Ce@MOR\_50 and (d) Ce@MOR\_50(IWI).

## TABLE CAPTIONS

Table S1. Catalytic performance of Ce@MOR\_X hybrids<sup>a</sup>

Table S2. Results for band deconvolution and assignment of transitions for DRUV spectra for MOR, Ce-MOR\_200(IWI), Ce@MOR\_X hybrids and CeO<sub>2</sub>. In parentheses, standard deviation for the average wavelength.

Table S3. Results for band deconvolution for Ce 3d XPS spectra measured on Ce-MOR\_200(IWI), Ce-MOR\_50(IWI) and Ce@MOR\_X hybrids. In parentheses, standard deviation for the binding energy.

Table S4. Results for band deconvolution for O 1s XPS spectra measured on Ce-MOR\_200(IWI), Ce-MOR\_50(IWI) and Ce@MOR\_X hybrids. In parentheses, standard deviation for the binding energy.

Table S5. Results for band deconvolution for the  $^{29}\text{Si}$ -NMR MAS spectra on the fresh MOR, Ce@MOR\_200, Ce@MOR\_50 and Ce-MOR\_50(IWI). In parentheses, standard deviation for the chemical shift.

Table S6. Acid site distribution and strength measured from NH<sub>3</sub>-TPD for the fresh and spent catalysts. Complete missing values.

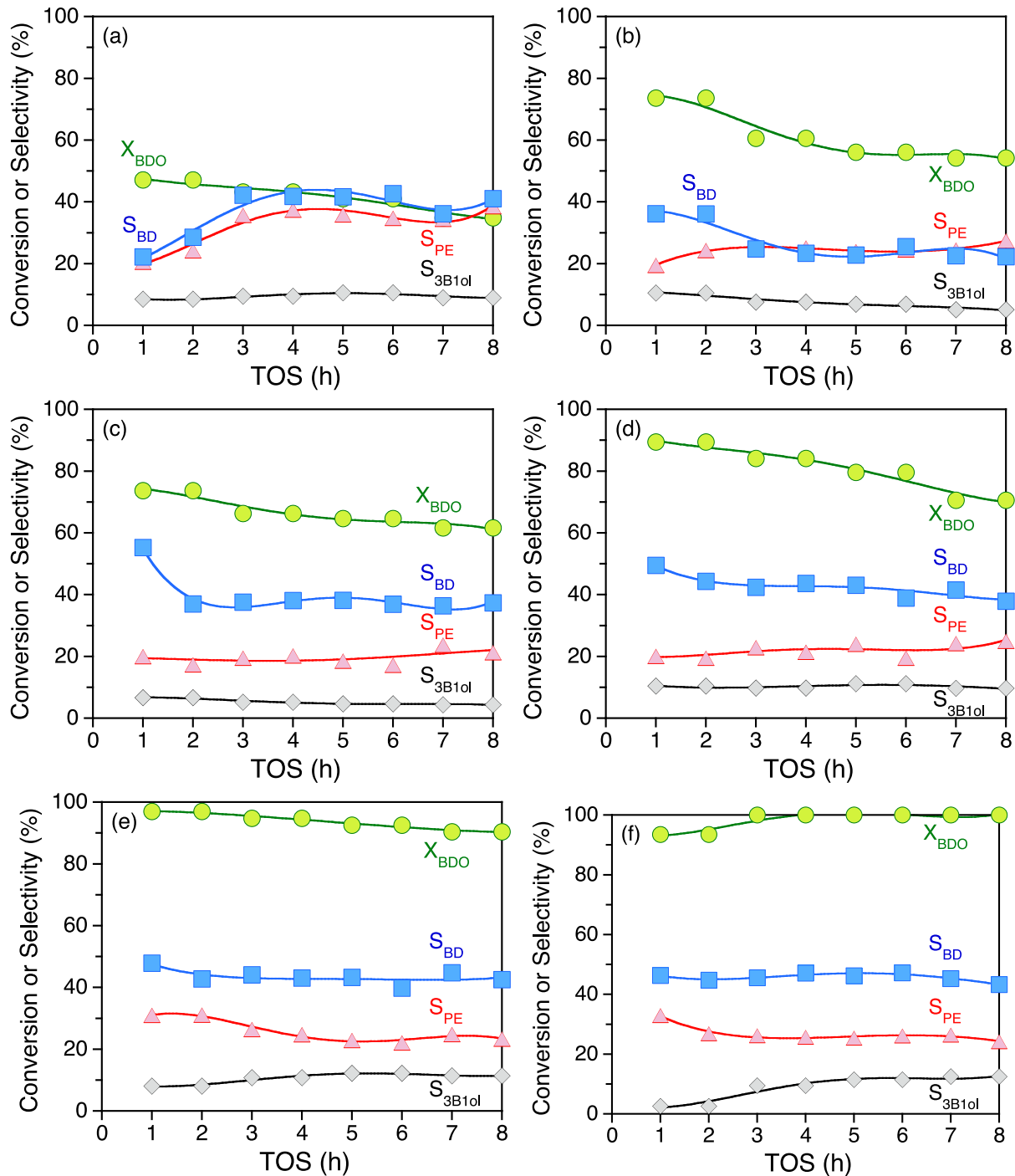


Figure S1. Evolution of the catalytic performance as a function of the time of stream (TOS) for: (a) MOR, (b) Ce-MOR\_200(IWI), (c) Ce-MOR\_50(IWI), (d) Ce@MOR\_200, (e) Ce@MOR\_100 and (f) Ce@MOR\_50. Nomenclature: X<sub>BDO</sub>, 1,3-BDO conversion; S<sub>BD</sub>, BD selectivity; S<sub>PE</sub>, propylene selectivity; S<sub>3B1ol</sub>, 3B1ol selectivity.

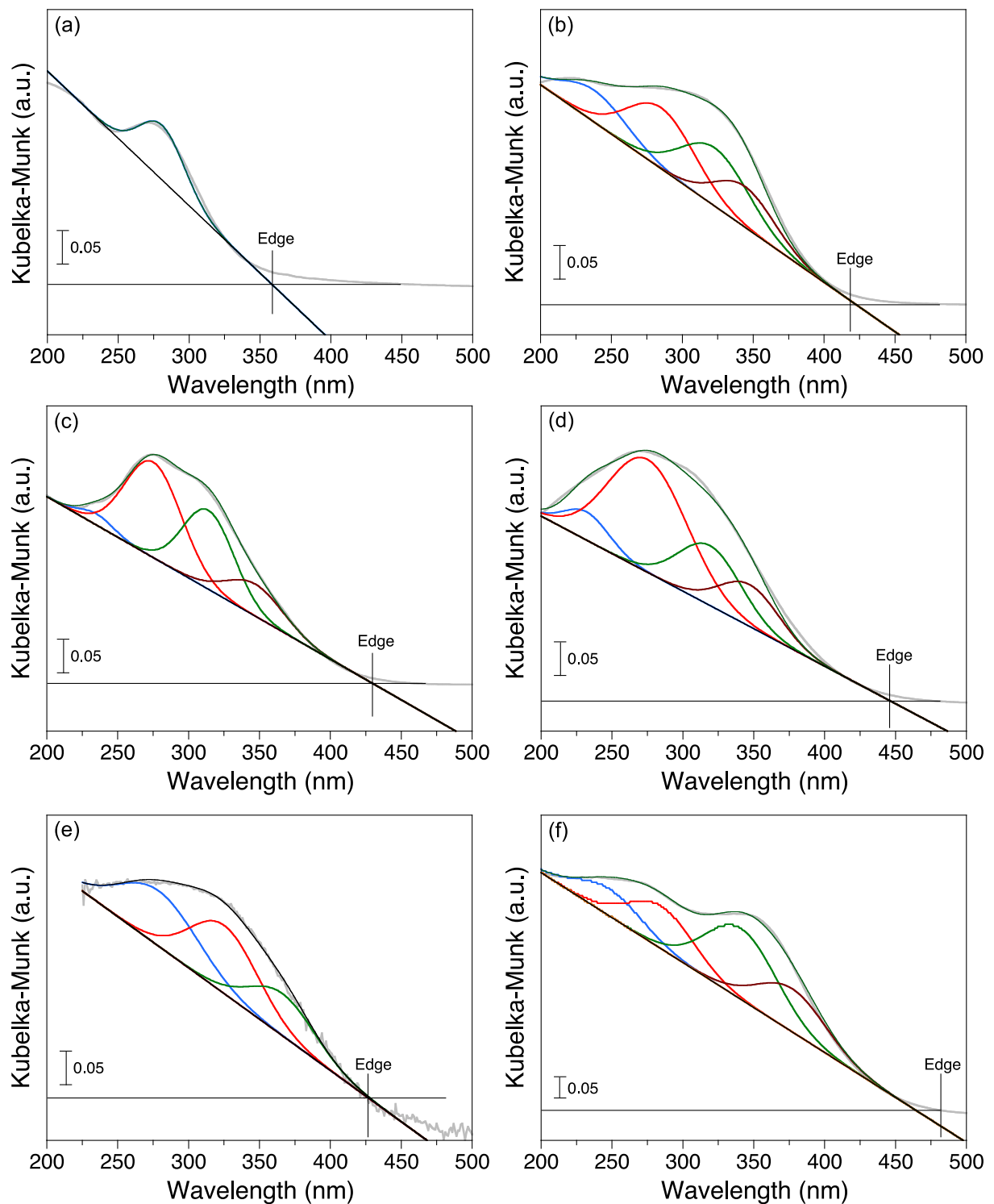


Figure S2. Band deconvolution for DRUV spectra: (a) MOR, (b) Ce-MOR\_200(IWI), (c) Ce@MOR\_200, (d) Ce@MOR\_50, (e) Ce@MOR\_20 and (f) CeO<sub>2</sub>.

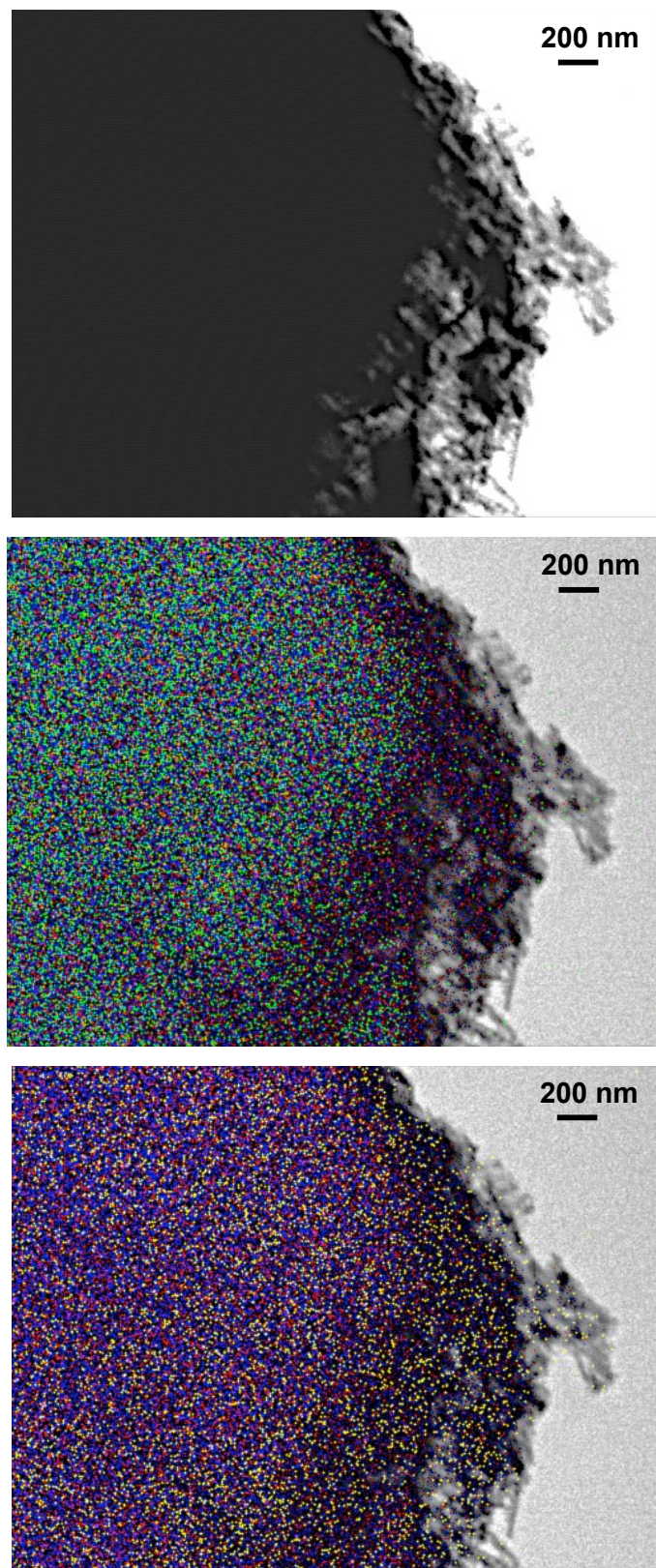


Figure S3. TEM-EDX images of Ce@MOR\_50 showing the location of Si (blue), Al (green), Ce (yellow) and O (magenta).

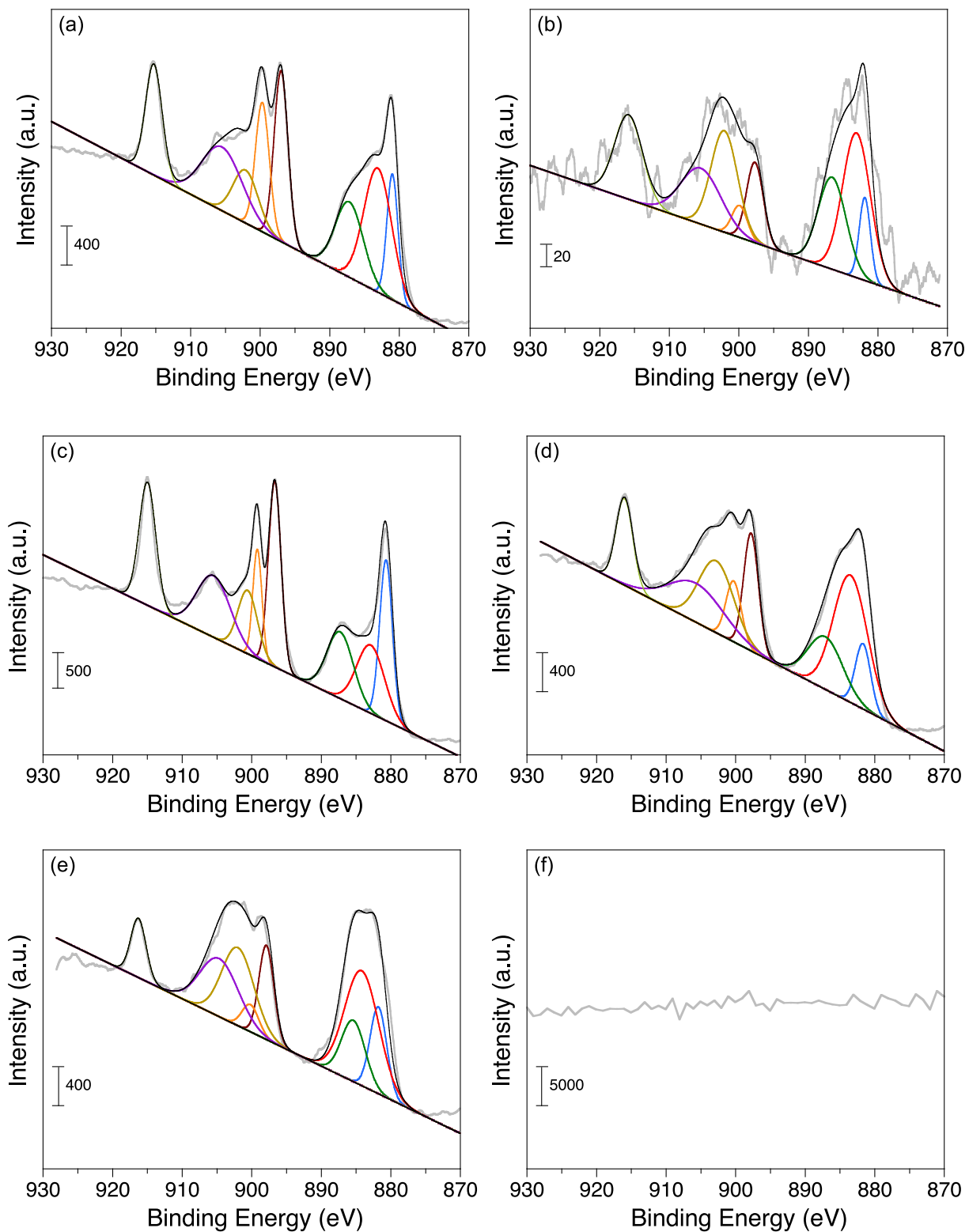


Figure S4. Band deconvolution for Ce 3d XPS spectra: (a) Ce-MOR\_200(IWI), (b) Ce@MOR\_200, (c) Ce-MOR\_50(IWI), (d) Ce@MOR\_50, (e) Ce@MOR\_20 and (f) MOR.

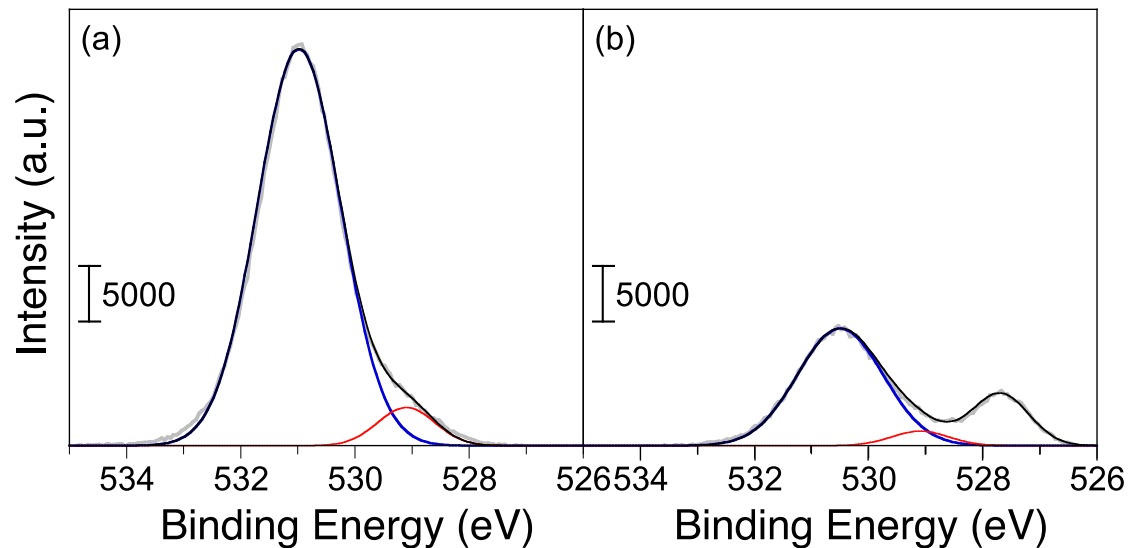


Figure S5. XPS spectra for: (a) Ce-MOR\_20 and (b) Ce@MOR\_50(IWI).

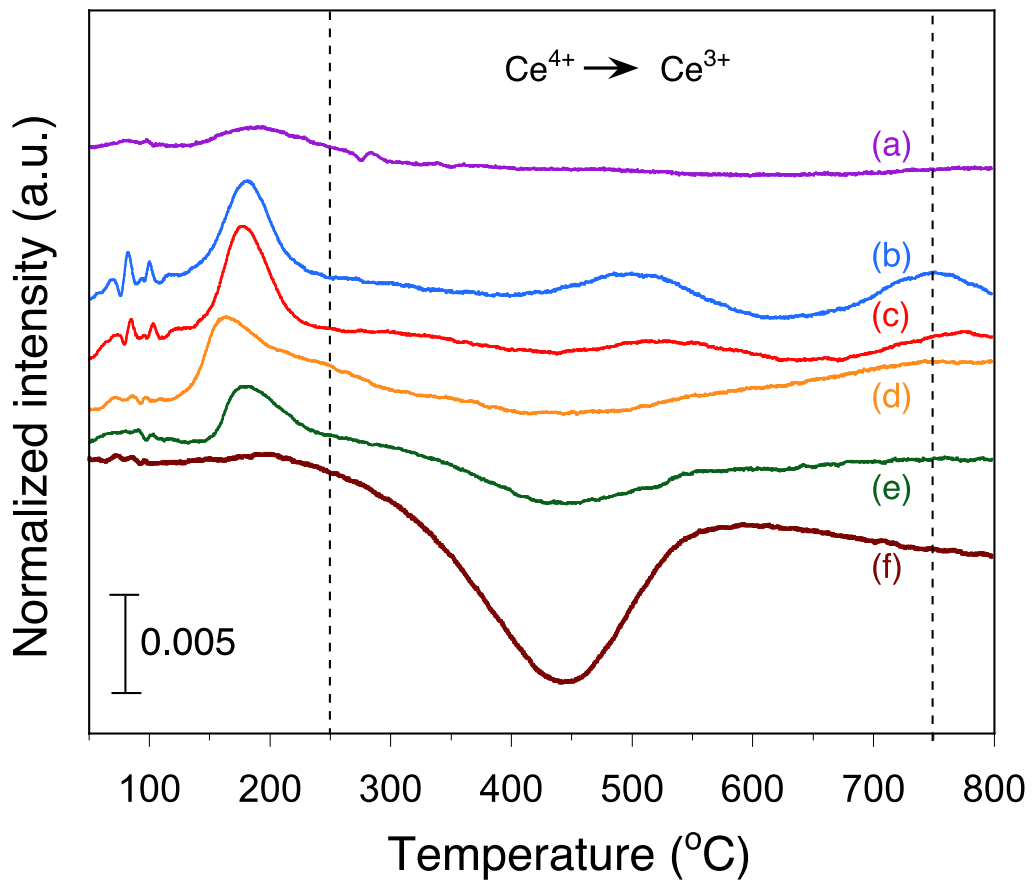


Figure S6. H<sub>2</sub>-TPR profiles for: (a) Ce@MOR\_50(IWI), (b) MOR, (c) Ce@MOR\_200, (d) Ce@MOR\_100, (e) Ce@MOR\_50 and (f) Ce@MOR\_20.

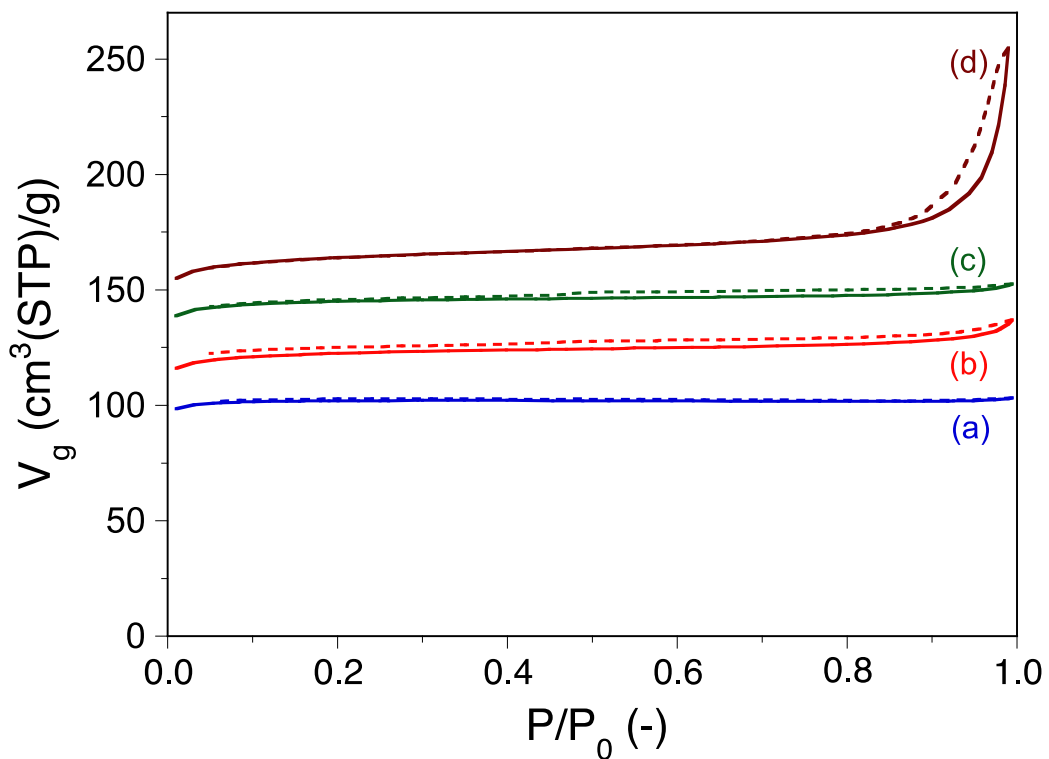


Figure S7. N<sub>2</sub> adsorption/desorption isotherms for: (a) MOR, (b) Ce@MOR\_200, (c) Ce@MOR\_100 and (d) Ce@MOR\_50.

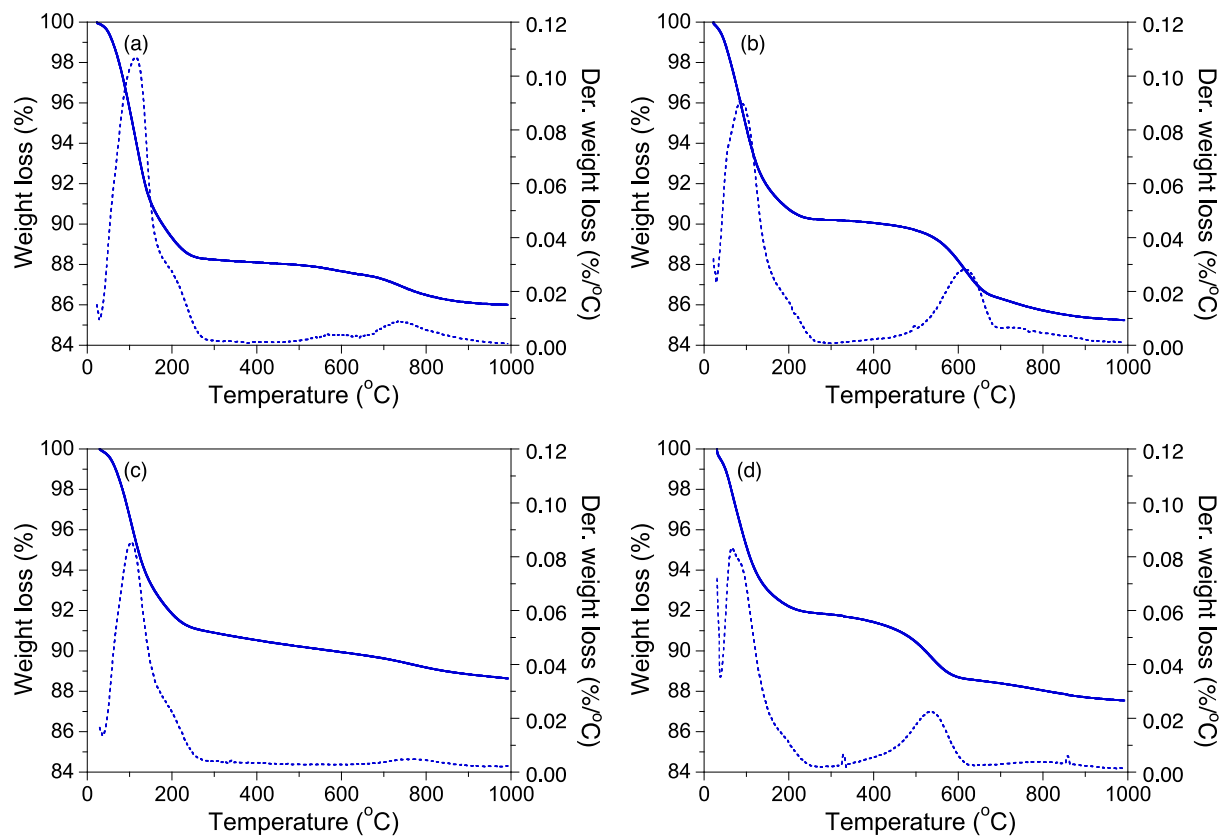


Figure S8. TGA / DTG profiles for the fresh and spent catalysts: (a) fresh MOR, (b) spent MOR, (c) fresh Ce@MOR\_100 and (d) spent Ce@MOR\_100.

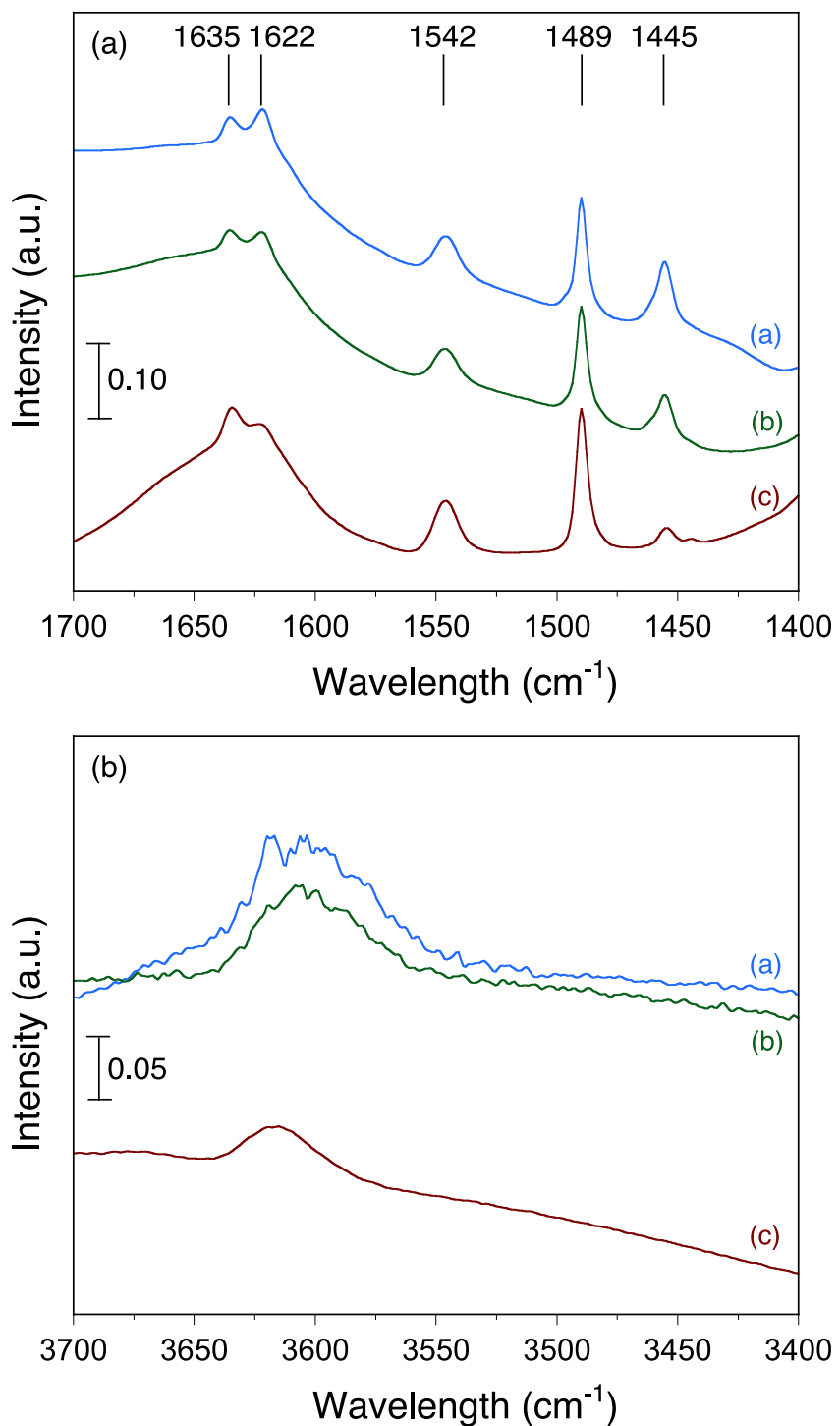


Figure S9. FT-IR absorption spectra after pyridine adsorption in the wavelength range of 1400-1700  $\text{cm}^{-1}$  (top) and 3400-3700  $\text{cm}^{-1}$  (bottom) for: (a) H-MOR, (b) Ce@MOR\_100 and (c) Ce@MOR\_50.

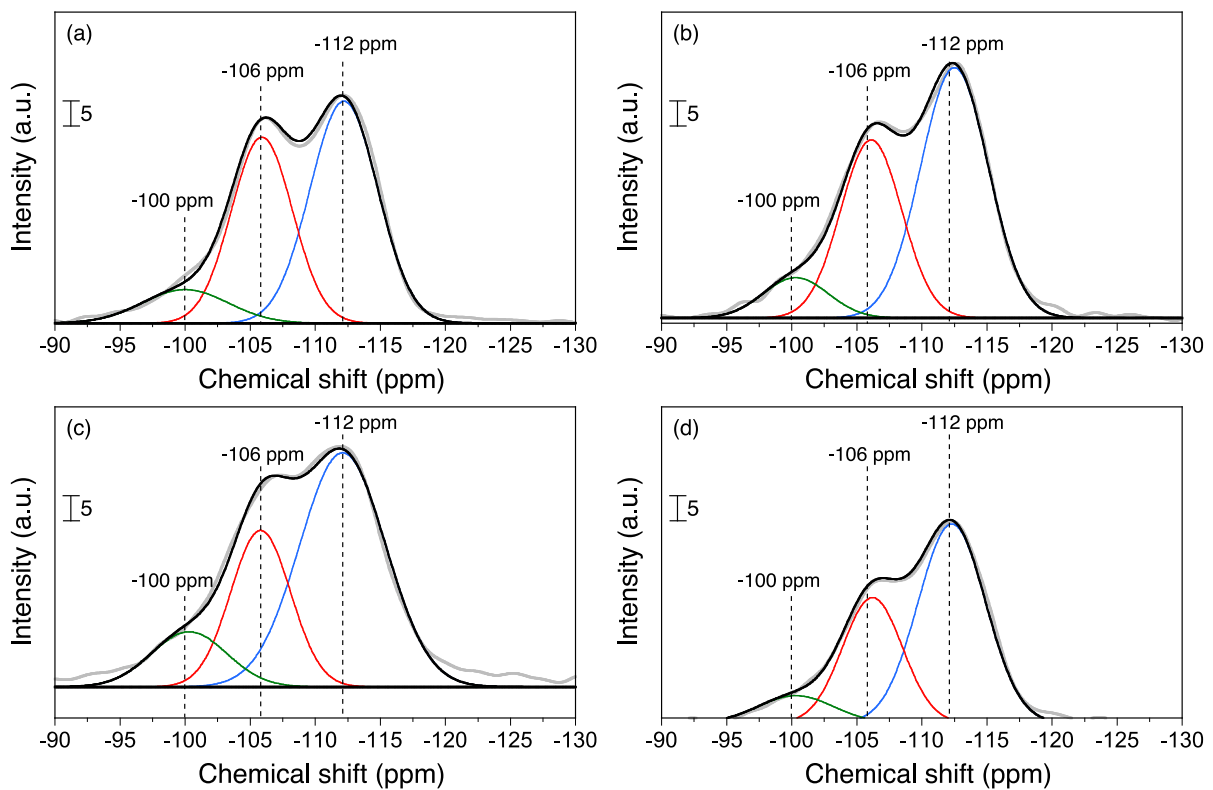


Figure S10. Deconvoluted  $^{29}\text{Si}$  NMR MAS spectra for: (a) MOR, (b) Ce@MOR\_200, (c) Ce@MOR\_50 and (d) Ce@MOR\_50(IWI).

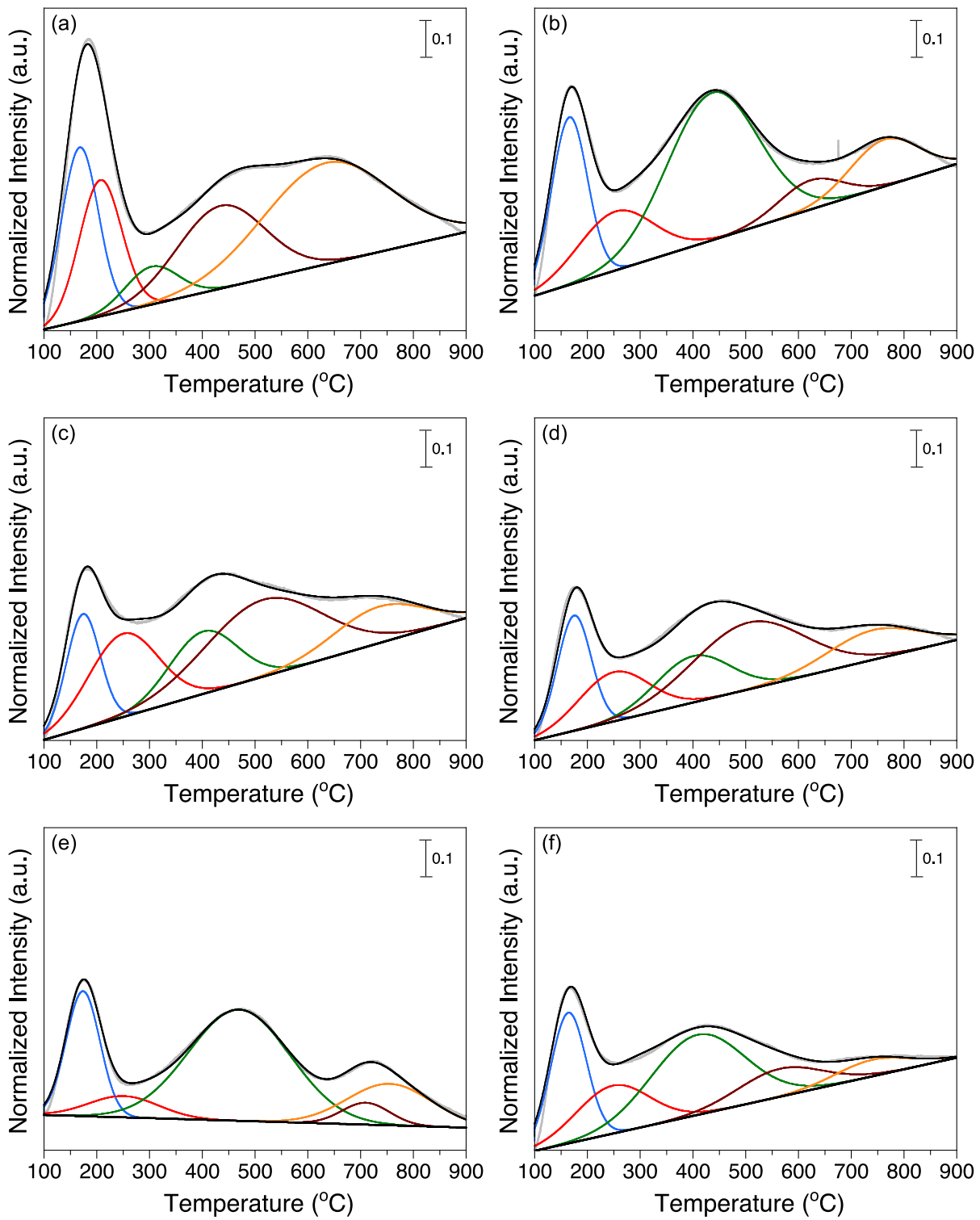


Figure S11. Deconvoluted  $\text{NH}_3$ -TPD profiles for the fresh catalysts: (a) MOR, (b) Ce@MOR\_200, (c) Ce@MOR\_100, (d) Ce@MOR\_50, (e) Ce@MOR\_200(IWI) and (f) Ce@MOR\_50(IWI).

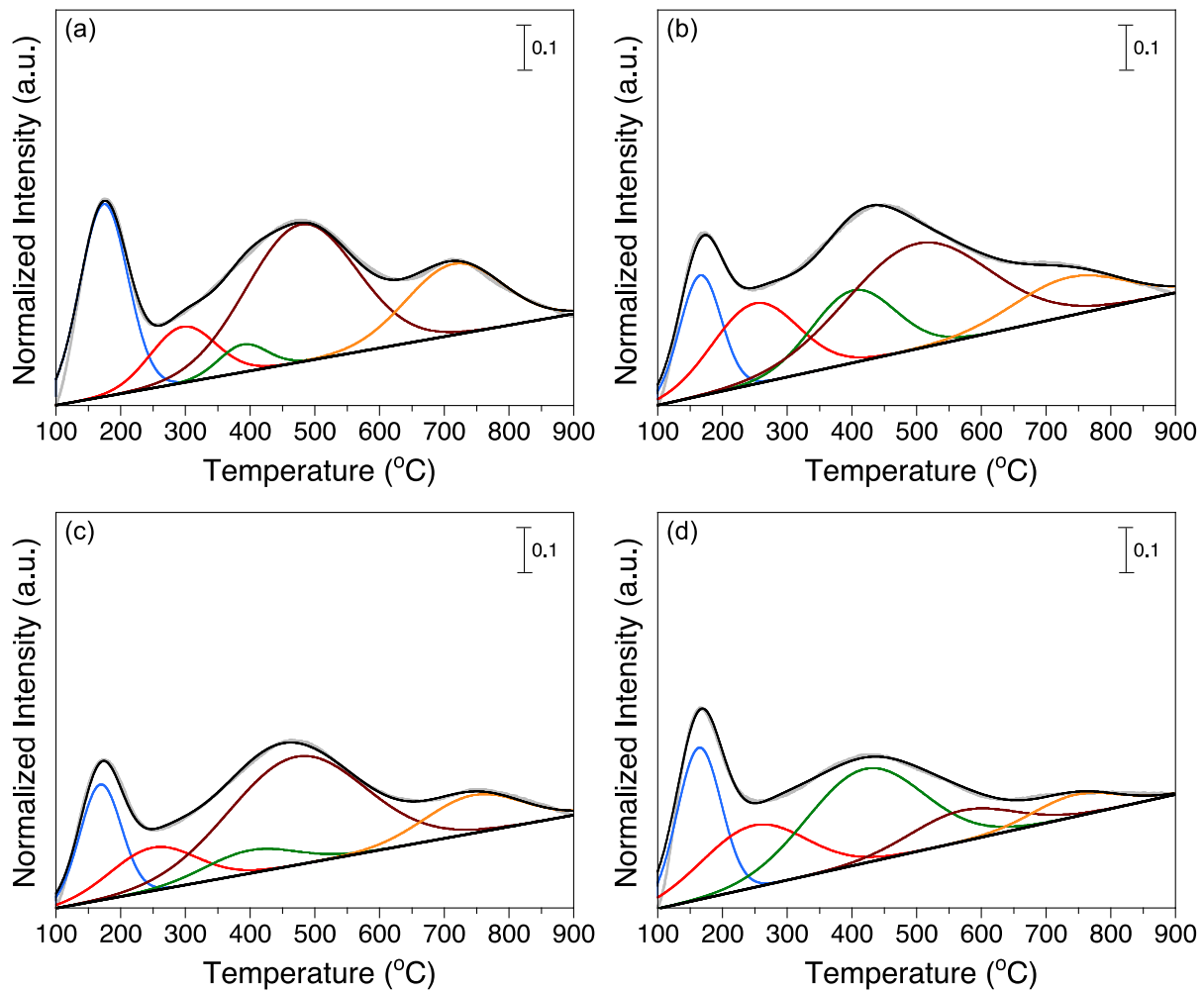


Figure S12. Deconvoluted  $\text{NH}_3$ -TPD profiles for the spent catalysts: (a) MOR, (b) Ce@MOR\_100, (c) Ce@MOR\_50 and (d) Ce@MOR\_50(IWI).

Table S1. Catalytic performance of SBA@X catalysts<sup>a</sup>

Catalyst	BDO conversion (%)	Yield (%) <sup>b</sup>			BD productivity (g <sub>BD</sub> .g <sub>cat</sub> <sup>-1</sup> .h <sup>-1</sup> )	C balance
		3B1ol	PE	BD		
MOR	38	9.8	13	16	1.32	0.95
MOR_200(IWI)	55	3.3	14	13	1.09	0.77
MOR_100(IWI)	67	3.7	12	22	1.81	0.75
MOR_50(IWI)	63	2.8	13	24	1.98	0.80
Ce@MOR_200	75	7.9	16	25	2.08	0.75
Ce@MOR_100	92	11	21	39	3.29	0.83
Ce@MOR_50	100	12	24	46	3.84	0.90
Ce@MOR_20	29	2.7	11	5.4	0.46	-

<sup>a</sup>Reaction conditions: 2.8 mL/h liquid flow, 60 mL(STP)/min carrier gas flow; 350 °C, 200 mg catalyst, 8 h time on stream, atmospheric pressure

<sup>b</sup>Other reaction products (<5% selectivity): MEK, *l*-butanol, 2-butanol, 3B2ol

Table S2. Results for band deconvolution and assignment of transitions for DRUV spectra for MOR, Ce-MOR\_200(IWI), Ce@MOR\_X hybrids and CeO<sub>2</sub>. In parentheses, standard deviation for the average wavelength

Conditions		Band I (O <sup>2-</sup> → Ce <sup>3+</sup> )	Band II (Blank)	Band III (O <sup>2-</sup> → Ce <sup>4+</sup> )	Band IV (Inter-band)
MOR	λ (nm)	-	281 (16)	-	-
	%	-	100%	-	-
Ce@MOR_200(IWI)	λ (nm)	238 (23)	285 (24)	323 (24)	344 (21)
	%	16%	33%	32%	19%
Ce-MOR_200	λ (nm)	235 (12)	275 (20)	314 (18)	347 (20)
	%	3.2%	46%	35%	16%
Ce@MOR_50	λ (nm)	234 (30)	272 (24)	314 (22)	352 (24)
	%	9.7%	50%	35%	5.8%
Ce@MOR_20	λ (nm)	-	279 (28)	325 (24)	366 (23)
	%	-	37%	40%	23%
CeO <sub>2</sub>	λ (nm)	248 (23)	285 (23)	341 (24)	377 (24)
	%	14%	22%	40%	24%

Table S3. Results for band deconvolution for Ce 3d XPS spectra measured on Ce-MOR\_200(IWI), Ce-MOR\_50(IWI) and Ce@MOR\_X hybrids. In parentheses, standard deviation for the binding energy.

Conditions		Band I	Band II	Band III	Band IV	Band V	Band VI	Band VII	Band VIII
Ce-MOR_50(IWI)	BE (eV)	880.7 (0.9)	882.9 (2.0)	887.3 (1.9)	896.7 (0.9)	899.2 (0.6)	900.6 (1.3)	905.5 (2.5)	915.0 (1.1)
	%	14%	13%	12%	16%	7.7%	8.4%	15%	14%
Ce-MOR_200(IWI)	BE (eV)	881.0 (0.8)	883.1 (2.0)	887.2 (2.0)	897.0 (1.0)	899.7 (1.0)	902.1 (1.8)	905.5 (2.9)	915.3 (1.2)
	%	8.2%	20%	12%	14%	11%	7.9%	15%	11%
Ce@MOR_200	BE (eV)	881.9 (0.8)	883.1 (2.0)	886.6 (2.0)	897.7 (1.2)	899.9 (1.1)	902.1 (1.9)	905.5 (2.9)	915.9 (2.0)
	%	5.5%	24%	15%	8.1%	2.9%	16%	14%	11%
Ce@MOR_50	BE (eV)	881.7 (1.1)	883.5 (2.4)	887.1 (2.5)	897.8 (1.1)	900.3 (1.1)	902.8 (2.5)	905.7 (4.0)	916.0 (1.2)
	%	6.3%	27%	11%	11%	5.8%	16%	14%	9.1%
Ce@MOR_20	BE (eV)	881.8 (1.2)	884.2 (2.4)	885.4 (1.7)	897.9 (1.1)	900.2 (1.2)	902.0 (2.3)	904.7 (2.8)	916.3 (1.1)
	%	10%	27%	10%	10%	3.2%	17%	16%	6.3%

Table S4. Results for band deconvolution for O 1s XPS spectra measured on MOR, Ce-MOR\_200(IWI), Ce-MOR\_50(IWI) and Ce@MOR\_X hybrids. In parentheses, standard deviation for the binding energy.

Conditions		Band I	Band II	Band III
MOR	BE (eV)	530.7 (0.8)	-	-
	%	100%	-	-
Ce-MOR_50(IWI)	BE (eV)	530.5 (0.8)	529.1 (0.5)	527.7 (0.5)
	%	72%	6%	22%
Ce-MOR_200(IWI)	BE (eV)	530.6 (0.8)	528.0 (0.6)	-
	%	93%	7%	-
Ce@MOR_200	BE (eV)	530.9 (0.8)	529.5 (0.9)	-
	%	95%	5%	-
Ce@MOR_50	BE (eV)	530.8 (0.8)	528.9 (0.8)	-
	%	94%	6%	-
Ce@MOR_20	BE (eV)	531.0 (0.7)	529.1 (0.5)	-
	%	94%	6%	-

Table S5. Results for band deconvolution for the  $^{29}\text{Si}$ -NMR MAS spectra on the fresh MOR, Ce@MOR\_200, Ce@MOR\_50 and Ce-MOR\_50(IWI). In parentheses, standard deviation for the chemical shift.

Conditions		Band I	Band II	Band III
MOR	$\delta$ (ppm)	-112.2 (2.6)	-105.9 (2.4)	-100.0 (3.3)
	%	51%	39%	9.8%
Ce@MOR_200	$\delta$ (ppm)	-112.5 (2.6)	-106.1 (2.4)	-100.3 (2.5)
	%	56%	36%	8.6%
Ce@MOR_50	$\delta$ (ppm)	-112.1 (3.3)	-105.8 (2.3)	-100.3 (2.9)
	%	60%	28%	12%
Ce-MOR_50(IWI)	$\delta$ (ppm)	-112.3 (2.6)	-106.2 (2.3)	-100.3 (2.9)
	%	58%	32%	9.0%

Table S6. Acid site distribution and strength measured from NH<sub>3</sub>-TPD for the fresh and spent catalysts. Nomenclature: L (low strength), M (medium strength), H (high strength).

Conditions	Band I (L)		Band II (L)		Band III (M)		Band IV (M / H)		Band V (H)	
	T <sub>M</sub> (°C) <sup>a</sup>	Φ <sub>NH<sub>3</sub></sub> (%)	T <sub>M</sub> (°C) <sup>a</sup>	Φ <sub>NH<sub>3</sub></sub> (%)	T <sub>M</sub> (°C) <sup>a</sup>	Φ <sub>NH<sub>3</sub></sub> (%)	T <sub>M</sub> (°C) <sup>a</sup>	Φ <sub>NH<sub>3</sub></sub> (%)	T <sub>M</sub> (°C) <sup>a</sup>	Φ <sub>NH<sub>3</sub></sub> (%)
MOR	168 (35)	18%	207 (40)	17%	304 (50)	5.9%	435 (83)	21%	635 (120)	37%
MOR_AR <sup>b</sup>	174 (37)	25%	296 (50)	10%	389 (37)	3.7%	479 (85)	42%	715 (74)	19%
Ce-MOR_200(IWI)	174 (32)	19%	251 (66)	6.8%	-	-	470 (96)	52%	755 (80)	21%
Ce-MOR_50(IWI)	164 (34)	30%	248 (69)	18%	409 (88)	39%	<b>565 (80)</b>	<b>12%</b>	740 (70)	6.4%
Ce-MOR_50(IWI)_AR <sup>b</sup>	164 (34)	23%	248 (80)	22%	420 (90)	38%	<b>570 (80)</b>	<b>11%</b>	745 (65)	6.4%
Ce@MOR_200	166 (34)	20%	253 (71)	15%	437 (86)	47%	<b>623 (60)</b>	<b>6.5%</b>	763 (65)	11%
Ce@MOR_100	174 (32)	15%	250 (66)	22%	402 (64)	16%	516 (110)	34%	736 (86)	12%
Ce@MOR_100_AR <sup>b</sup>	166 (32)	13%	250 (66)	18%	402 (64)	16%	501 (110)	41%	736 (86)	11%
Ce@MOR_50	175 (32)	19%	250 (66)	16%	400 (70)	17%	505 (105)	36%	742 (86)	13%
Ce@MOR_50_AR <sup>b</sup>	169 (32)	16%	250 (66)	13%	400 (70)	7.2%	472 (105)	51%	745 (75)	12%

<sup>a</sup>T<sub>M</sub> = mean temperature; in parentheses, standard deviation (°C)

<sup>b</sup> AR = After reaction (spent catalysts)